Sensors and Actuators B 146 (2010) 28–34

Contents lists available at ScienceDirect

Sensors and Actuators B: Chemical

journal homepage: www.elsevier.com/locate/snb

Fabrication of NO_x gas sensors using In_2O_3–ZnO composite films

Chia-Yu Lin[a], Yueh-Yuan Fang[b], Chii-Wann Lin[b,c], James J. Tunney[d], Kuo-Chuan Ho[a,e,*]

[a] Department of Chemical Engineering, National Taiwan University, Taipei 10617, Taiwan
[b] Institute of Biomedical Engineering, National Taiwan University, Taipei 10617, Taiwan
[c] Institute of Electrical Engineering, National Taiwan University, Taipei 10617, Taiwan
[d] Institute for Chemical Process and Environmental Technology, National Research Council of Canada, Ottawa K1A 0R6, Canada
[e] Institute of Polymer Science and Engineering, National Taiwan University, Taipei 10617, Taiwan

ARTICLE INFO

Article history:
Received 26 June 2009
Received in revised form 11 February 2010
Accepted 12 February 2010
Available online 19 February 2010

Keywords:
Gas sensor
Indium oxide
In_2O_3–ZnO
Nitric oxide
Zinc oxide

ABSTRACT

In_2O_3–ZnO composite films were fabricated and their NO_x sensing characteristics were investigated in this study. The content of ZnO in In_2O_3–ZnO film was controlled by adjusting the Zn^{2+}/In^{3+} molar ratio (r) during the film preparation. With suitable amount of ZnO incorporated into the In_2O_3 films, the responses of the composite films to NO_x at operation temperatures below 200 °C were greatly improved. However, as the ZnO content was further increased, the grain of the composite film started to merge into big ones, thus decreasing the surface area and resulting in lower sensor responses. The detection limit ($S/N = 3$) of In_2O_3–ZnO composite film ($r = 0.67$) reached 12 ppb at 150 °C. Both pure In_2O_3 ($r = 0$) and In_2O_3–ZnO composite films ($r = 0.67$) showed no response to CO gas.

1. Introduction

Sensors for detecting low concentration of nitric oxide (NO) have received progressive attention due to its environmental and health-related importance. NO gas, released from the combustion processes, not only is a precursor of the acid rain, but also is the cause for the depletion of ozone [1]. In the presence of excess oxygen, NO will be oxidized to nitrogen dioxide (NO_2), with the reaction time depending on the NO concentration in air. Frequent exposure to the mixture of NO and NO_2 gas (NO_x) would cause pulmonary edema and fatality. According to the regulations set by the Occupational Safety and Health Administration (OSHA), the permissible exposure limit for NO is at 25 ppm (TWA). It also has been reported that NO has effects on neuron functions, such as transcriptional regulation and ion channel functions, and thus change in NO levels can signify neuron death which is induced by neurodegenerative diseases [2]. Moreover, the exhaled NO concentration has been identified as a biomarker for airway inflammation such as asthma [3] and bronchiectasis [4]. Generally, the exhaled NO level of the patients with asthma is about 34.7–51.1 ppb, which is 3–4 times higher than that of healthy people [3]. It is, therefore, necessary to develop rugged and reliable NO gas sensors capable of making real-time measurements for public health and security applications.

Solid-state gas sensors, based on thin film's conductivity changes upon interaction with target gas molecules, have widely used as the platform for the detection of some gas molecules. Among the materials used, In_2O_3 is known to be sensitive to some oxidizing gases, such as NO_x [5–8,16] and ozone [9,10]. In order to improve the sensor sensitivity, nanostructured In_2O_3 [11,12] or binary oxide films [13,14] have been used. On the other hand, zinc oxide (ZnO) also has been proposed as a sensing material for the detection of some pollutants [15,16]. Besides, ZnO has been reported as an effective dopant to improve the sensor sensitivity. Yu and Choi [17] reported that the microstructure of SnO_2 was modified after incorporating zinc oxide, resulting in the improvement of sensor sensitivity toward carbon monoxide. Moreover, Miyata et al. [18] reported that the enhanced sensitivity of In_2O_3 based CCl_4 sensor was related to the formation of $Zn_2In_2O_3$ phase.

In this study, ZnO was used as the doping material of In_2O_3 for enhancing NO_x gas sensing performance. Various amounts of ZnO were incorporated into In_2O_3 film via co-precipitating method. The effect of Zn^{2+}/In^{3+} (r) ratio during the preparation on the responses of the composite films toward NO_x was investigated. The results showed that the incorporation of ZnO into the In_2O_3 film can improve the composite film's sensitivity of the In_2O_3 film to NO_x gas at low operation temperature (<200 °C).

* Corresponding author at: Department of Chemical Engineering, National Taiwan University, No. 1, Sec. 4, Roosevelt Rd., Taipei city 10617, Taiwan.
Tel.: +886 2 2366 0739; fax: +886 2 2362 3040.
E-mail address: kcho@ntu.edu.tw (K.-C. Ho).

0925-4005/$ – see front matter © 2010 Elsevier B.V. All rights reserved.
doi:10.1016/j.snb.2010.02.040

Table 1
The film thickness and the actual In/Zn ratio of the In_2O_3–ZnO composite films with different values of *r*.

	r values				
	0.00	0.33	0.50	0.67	1.00
Film thickness (μm)	3.83 ± 0.49	3.28 ± 0.62	4.00 ± 1.03	4.75 ± 0.41	4.00 ± 0.35
Actual Zn/In molar ratio	0.00	0.09	0.14	0.25	0.34

2. Experimental

2.1. Preparation of In_2O_3–ZnO films

The mixture of $In(OH)_3$ and $Zn(OH)_2$ was formed by carrying out the chemical bath precipitation at 90 °C for 1 h in an aqueous solution containing $InCl_3$, $Zn(NO_3)_2$, and hexamethylenetetramine (HMT). To synthesize $In(OH)_3$–$Zn(OH)_2$ with different molar ratios, various amounts of 25 mM $Zn(NO_3)_2$ solution were added in a 25 mM aqueous solution of $InCl_3$, *i.e.*, with different Zn^{2+}/In^{3+} molar ratios (*r*). The concentration of HMT used was 25 mM, and the molar ratio of the sum of Zn^{2+} and In^{3+} ions source to HMT was kept at 1:1.

Thereafter, the In_2O_3–ZnO composite films were fabricated by dropping 60 μl of the $In(OH)_3$–$Zn(OH)_2$ solutions with different *r* values on the gold interdigitated electrodes ($n = 24$ fingers, 50 μm spaced, 6 mm long and 50 μm wide). Then the films were dried at room temperature and annealed at 500 °C for 30 min under pure O_2 atmosphere.

2.2. Gas sensing experiment

The electrodes were mounted onto a heater and inside a chamber equipped with gas-flow manifold and mass flow controller (Protec Instruments, Inc.). The mass flow controller offers ±1% full-scale accuracy. The apparatus facilitated automated (PC-DOS) control of temperature and data acquisition of the film resistance using a 2-wire method with a Hewlett Packard 34401A digital voltmeter which permitted resistance (*R*) measurements in the range $0 < R < 120\ M\Omega$. Various concentrations of NO_x were tuned by changing the ratio of the flow rate of 484 ppm NO stream (Praxair Inc.) to that of a zero-grade air stream (BOC Canada Ltd.), and were delivered to the chamber at an overall flow rate of 200 $cm^3\ min^{-1}$. Since some part of NO would oxidize to NO_2 under air [28], we use NO_x to represent the mixture of NO and NO_2. To clean the surface of the In_2O_3–ZnO films, the In_2O_3–ZnO films were thermally treated from 100 to 500 °C at a heating rate of 10 °C min^{-1} under zero-grade air environment for 5 cycles.

The response, *S*, is defined by the following equation:

$$S = \frac{R_g - R_{air}}{R_{air}} \quad (1)$$

where R_{air} and R_g are the resistances of the film in zero-grade air gas and in test gas, respectively.

The microstructure of In_2O_3–ZnO composites and the amount of ZnO incorporated into the composites were determined by using a JEOL 840 A scanning electron microscope and an X-ray recorded on a PHI 5000 VersaProbe (ULVAC-PHI, Chigasaki, Japan) system using a microfocused (100 μm, 25 W) Al X-ray beam, respectively. All photos were taken using an accelerating voltage of 30 kV. The thicknesses of the composite films were determined by cross-sectional SEM. The crystalline phase of the In_2O_3–ZnO films was determined using a General Area Detector Diffraction System (Bruker AXS GADDS) with Co Kα radiation.

3. Results and discussion

3.1. Characterization of In_2O_3 or In_2O_3–ZnO films

The content of ZnO in In_2O_3–ZnO composite film was controlled by adjusting the Zn^{2+}/In^{3+} (*r*) ratio during the preparation, and the actual contents of ZnO in the composite film were measured by EDX. The actual Zn/In molar ratio along with the film thickness, prepared using different *r* values, are summarized in Table 1. It was found that the actual Zn/In molar ratio is much lower than that during the preparation, which is possibly resulted from much lower solubility constant of $In(OH)_3$ than that of $Zn(OH)_2$ ($1 \times 10^{-34}\ M^4$ vs. $3 \times 10^{-17}\ M^3$, 25 °C).

The surface morphology of the ZnO–In_2O_3 composite film is quite different from that of the pure In_2O_3 film. As shown in Fig. 1 (a)–(e), the In_2O_3–ZnO composite films showed a bimodal grain size distribution with a major fine and a minor coarse component. The amount, or density, of the coarse component increased as the value of *r* was increased. Fig. 2 shows the top-view of SEM images for the In_2O_3–ZnO composite, prepared with different *r* values, with lower magnification. It can be seen that the coarse component started to merge into bigger ones as the value of *r* was increased from 0.67 to 1.50. This change in the film surface morphology would influence the sensor response, which is discussed in Section 3.2. The growth of the coarse component presumably was resulted from the increase of the Zn^{2+} concentration, namely, the increase of the *r* value, since the precursor concentration would affect the size of the resultant ZnO particles [19].

Fig. 3 shows the X-ray diffraction of the In_2O_3–ZnO films with different *r* ratios. It was found that after the incorporation of ZnO, the rhombohedral phase of In_2O_3 was induced. Besides, the Wurtzite phase of ZnO was observed as *r* value was higher than 0.67.

3.2. Gas sensing characteristics

Fig. 4 shows the gas sensing responses of the composite films to 10 ppm NO_x at different operation temperatures. Note that R_{NO_x}/R_{air} stands for the ratio of the film resistance in the presence of 10 ppm NO_x to the film resistance in zero-grade air atmosphere. It was found that the responses of all composite films increased as the operation temperature was lowered. Besides, the Zn^{2+}/In^{3+} ratio (*r*) has great influence on the sensing responses of the composite films. The sensor response to NO gas, at the operation temperature lower than 200 °C, was much improved as *r* value was increased from 0.33 to 0.67. The grain sizes (*d*) of cubic In_2O_3, rhombohedral In_2O_3, and ZnO, estimated by using the XRD data of Fig. 3 and Scherrer's formula (Eq. (2)), are summarized in Table 2.

$$d = \frac{\lambda}{B\cos\theta} \quad (2)$$

where λ and *B* are the wavelength of the X-ray wavelength and full-width at half maximum intensity, respectively.

It was found that the grain size of the cubic In_2O_3 increased from 28.8 to 32.3 nm, as a small quantity of ZnO was incorporated into In_2O_3 film ($r = 0.33$), and decreased from 32.3 to 15.4 nm as the

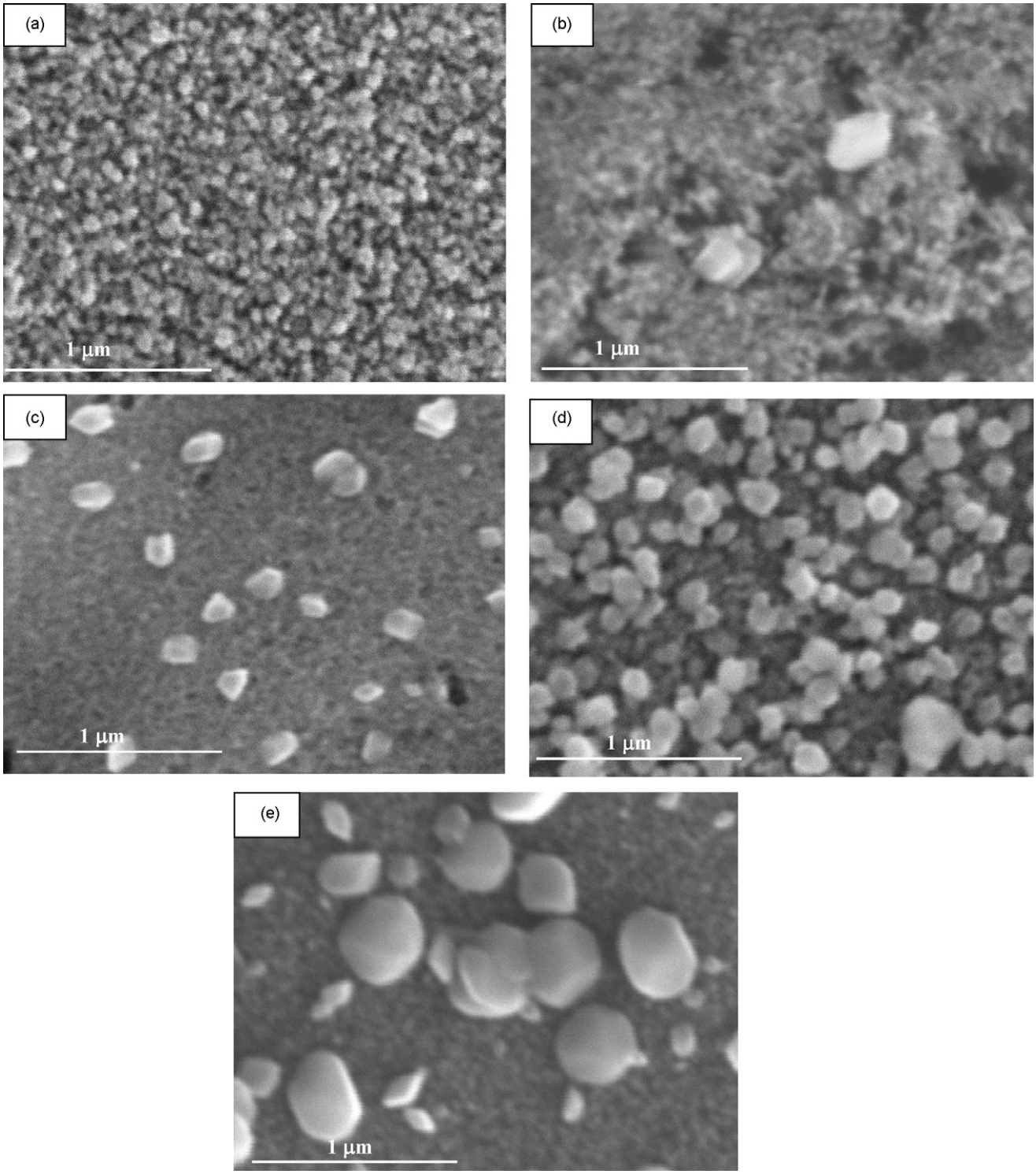

Fig. 1. The top-view of SEM images for the In_2O_3–ZnO composite film with r values of (a) 0, (b) 0.33, (c) 0.50, (d) 0.67, and (e) 1.00. Scale bar: 1 μm.

content of ZnO was further increased ($0.33 \leqq r \leqq 0.67$). It has been reported that the grain size has great influence on the sensitivity of the In_2O_3 based NO_2 gas sensor [20], and therefore the decrease in the grain size of In_2O_3 ($0.33 \leqq r \leqq 0.67$), resulted from the incorporation of ZnO, is one of the factors in enhancing the sensor response. However, as the content of ZnO was further increased ($r = 1$), the sensor responses at temperatures lower than 200 °C decreased, which could be due to the increase in the grain size of cubic In_2O_3 and the change in the microstructure (see Fig. 2). As a consequence, the optimal r value selected for the later experiments was 0.67.

It is interesting to note that NO_x gas can act as reducing gas at higher temperature and as oxidizing gas at lower temperature, and the response transition temperature ranges, as judged by the transition of R_{NO_x}/R_{air} value from greater than 1.0 to smaller than 1.0, depended on the r value. The results are summarized in Table 3. However, the transition in the sensor response was not observed

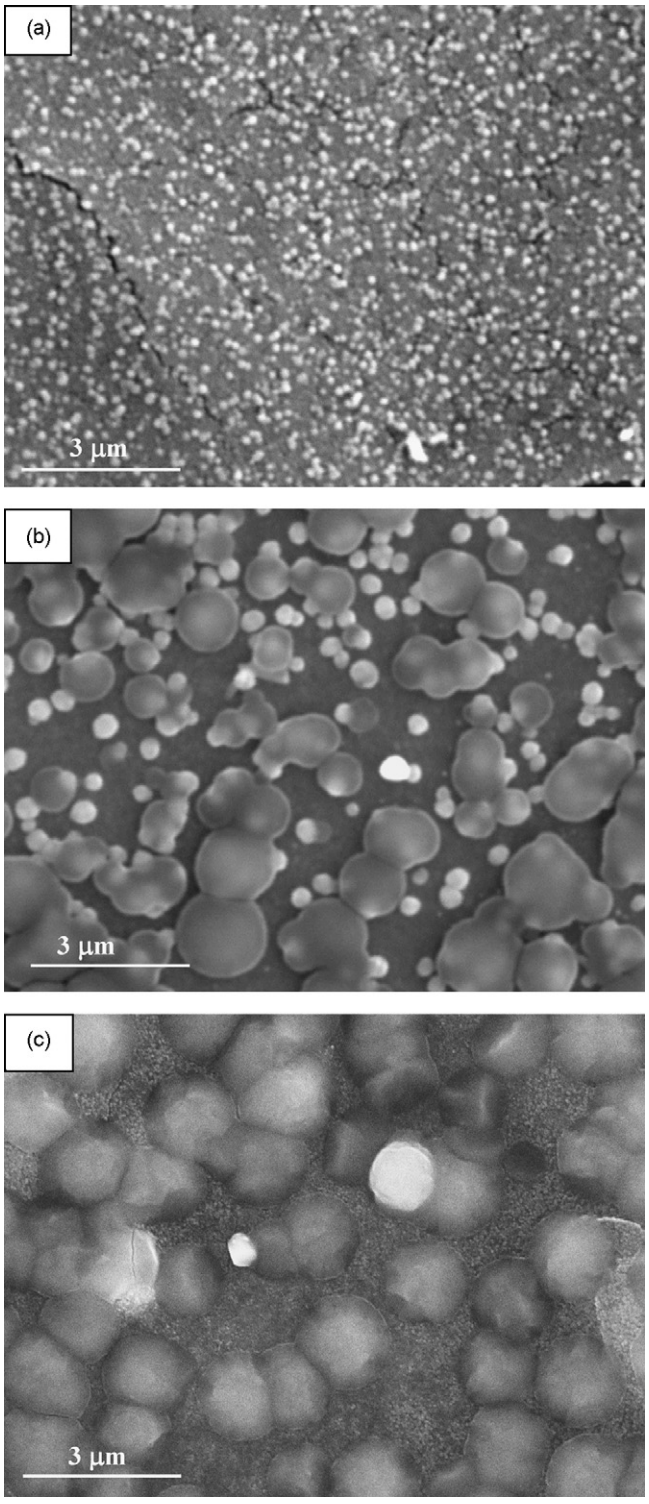

Fig. 2. The top-view of SEM images for the In_2O_3–ZnO composite film with *r* values of (a) 0.67, (b) 1.00, and (c) 1.50. Scale bar: 6 μm.

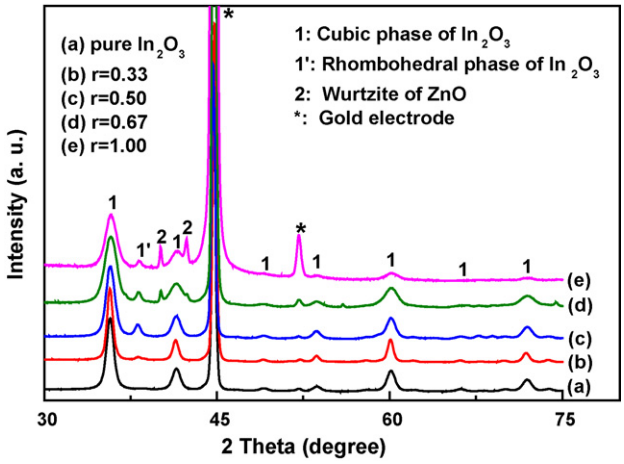

Fig. 3. The XRD patterns of the In_2O_3–ZnO films with different *r* ratios.

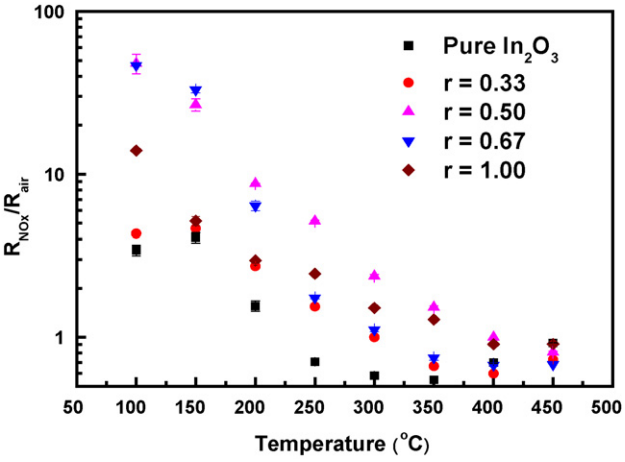

Fig. 4. The changes in the film resistance ratio (R_{NO_x}/R_{air}) for the pure In_2O_3 and In_2O_3–ZnO composite films with different Zn^{2+}/In^{3+} ratios. All films were exposed to 10 ppm NO in zero-grade air at different operation temperatures.

Table 2
The grain sizes of the cubic In_2O_3, rhombohedral In_2O_3, and ZnO in the In_2O_3–ZnO composite films with different values of *r*.

	r values				
	0.00	0.33	0.50	0.67	1.00
Grain size of In_2O_3[a] (nm)	28.8	32.3	22.2	15.4	17.6
Grain size of In_2O_3[b] (nm)	N.D.	25.1	26.2	34.1	32.8
Grain size of ZnO (nm)	N.D.	N.D.	N.D.	55.8	61.2

[a] Cubic phase.
[b] Rhombohedral phase.

3.3. Possible sensing mechanisms

At temperature lower than the transition temperature, the oxygen ions (O_{2ads}^-) would form at the surface of the In_2O_3 film in a

in the interested temperature range as background zero-grade air was replaced with N_2 (see Fig. 5). Note that R_{NO}/R_{N_2} stands for the ratio of the film resistance in the presence of 10 ppm NO to the film resistance in N_2 atmosphere. Since the transformation of NO into NO_2 under N_2 atmosphere is negligible, we use NO instead of NO_x here. Therefore, it can be inferred that the transition in the sensor response is strongly related to the presence of oxygen. The possible mechanisms are discussed in Section 3.3.

Table 3
The response transition temperature range for the In_2O_3–ZnO composite films with different values of *r*.

r values	Transition range (°C)
0.00	200–250
0.33	250–300
0.50	400–450
0.67	300–350
1.00	350–400

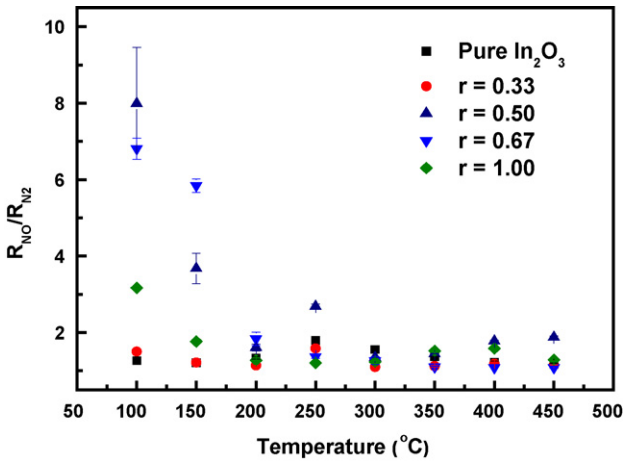

Fig. 5. The changes in the film resistance ratio (R_{NO}/R_{N_2}) for the pure In_2O_3 and In_2O_3–ZnO composite films with different Zn^{2+}/In^{3+} ratios. All films were exposed to 10 ppm NO in N_2 at different operation temperatures.

sequence of physisorption and charge exchange reactions with the bulk of In_2O_3 grain, as described by Eq. (3). After the In_2O_3–ZnO film was exposed to NO_x gas, NO_x would react with O_{2ads}^-, via Eqs. (4) and (5), and cause the reduction in the electron concentration, resulting in the increase in the sensor resistance [21].

$$O_2 + e^- \rightarrow O_{2ads}^- \quad (3)$$

$$NO_2 + O_{2ads}^- + 2e^- \rightarrow NO_{2ads}^- + 2O_{ads}^- \quad (4)$$

$$NO + O_{2ads}^- + e^- \rightarrow NO_{2ads}^- + O_{ads}^- \quad (5)$$

On the other hand, the adsorbed oxygen ion transformed into atomic oxygen ion (O_{ads}^-), as described by Eq. (6), when the operation temperature was increased to be higher than the transition temperature. After the In_2O_3–ZnO film was exposed to NO_x gas, NO_x would react with O_{ads}^-, via Eqs. (7) and (8), and cause the increase in the electron concentration, thus lowering the film resistance [22].

$$O_{2ads}^- + e^- \rightarrow 2O_{ads}^- \quad (6)$$

$$NO_2 + O_{ads}^- + 2e^- \rightarrow NO_{ads}^- + 2O_2 + e^- \quad (7)$$

$$NO + O_{ads}^- \rightarrow NO_2 + e^- \quad (8)$$

As the background zero-grade air was replaced with N_2 gas, the increase in the sensor resistance, as exposed to NO, was simply caused by the NO adsorption in the charged form (NO_{ads}^-) [23], as described by Eq. (9). Since no oxygen exists in N_2 gas, the possibility on the conversion of NO to NO_2 is excluded.

$$NO + e^- \rightarrow NO_{ads}^- \quad (9)$$

Although the transition behavior has been reported [24], the actual mechanism responsible for this phenomena remains to be clarified. On the other hand, it can also be found from Fig. 3 and Fig. 5 that the response of the In_2O_3–ZnO films to 10 ppm NO_x in zero-grade atmosphere is larger than that to 10 ppm NO in N_2 atmosphere. As it will be shown latter (Fig. 7), the responses of the pure In_2O_3 film to NO and NO_2 were about the same, but the response of the In_2O_3–ZnO film to NO_2 was higher than to NO_x. As a sequence, the difference in the sensor response at different atmospheres could be attributed to higher response of the In_2O_3–ZnO film to NO_2 or difference in the sensing mechanism behind. It should also be noted that although the recovery time and response time for In_2O_3–ZnO films became much faster as they were exposed to the reducing NO gas at temperatures higher than the transition temperature, the responses were quite small.

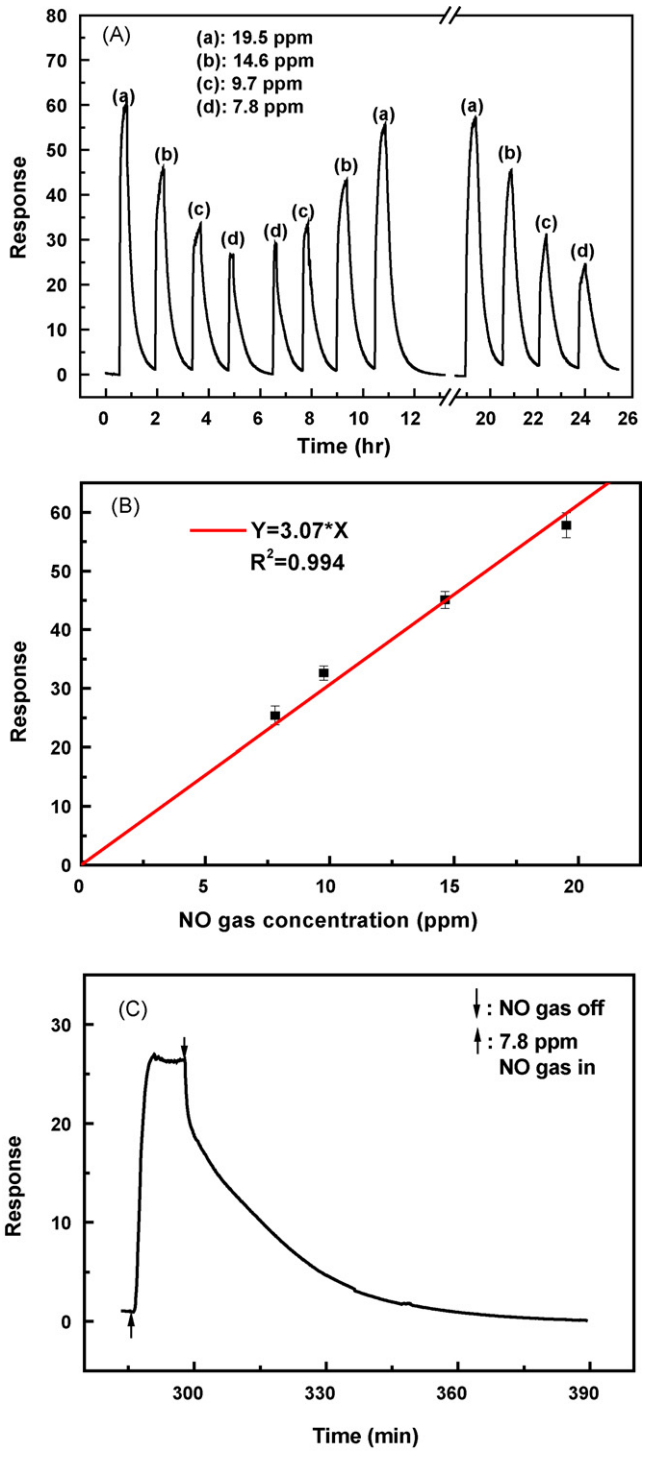

Fig. 6. (a) The transient responses for In_2O_3–ZnO ($r = 0.67$) composite film at 150 °C to various NO_x concentrations ranging from 7.8 to 19.5 ppm. (b) The resulted calibration curve. (c) The transient response of In_2O_3–ZnO ($r = 0.67$) composite film at 150 °C to 7.8 ppm.

3.4. NO_x sensing and interference

To develop the NO gas sensor with higher sensitivity and reasonable response and recovery times, we focused on the sensor response at temperature at 150 °C. Fig. 6(a) shows the dynamic responses of the In_2O_3–ZnO film ($r = 0.67$) to various concentrations of NO_x gas at 150 °C. It was found that all the responses are linear with the increase in the concentration of NO_x (Fig. 6(b)). The

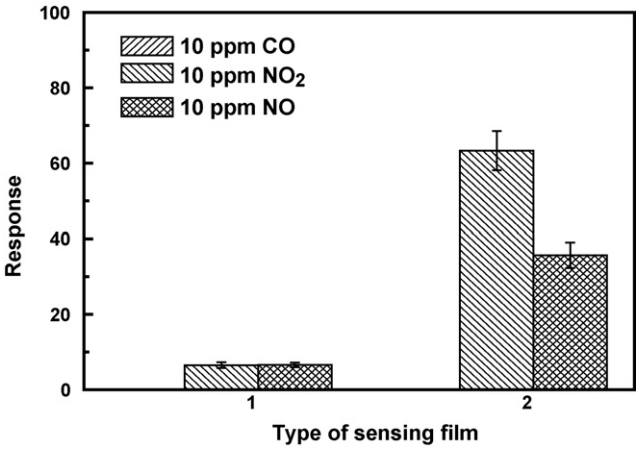

Fig. 7. The responses of the pure In_2O_3 (Type 1) and In_2O_3–ZnO ($r = 0.67$, Type 2) films against 10 ppm of NO_x, NO_2 and CO at 150 °C.

limit of detection, based on signal-to-noise ratio of 3, was found to be 12 ppb, which is much lower than that reported in the literature [25]. Moreover, the response time (t_{95}), defined as the time required to reach the 95% of the stable response to NO_x gas, and the recovery time (t_{95}), defined as the time required to reach the 95% of the baseline, for the sensor to detect 7.8 ppm were about 3.5 and 45 min, respectively (see Fig. 6(c)), which are comparable with some In_2O_3 based NO_x gas sensors [25,26]. The long response time and recovery time could be resulted from the low operation temperature [26] and/or the nature of the thick sensing film [27].

The interfering effects of CO and NO_2 were also examined. Fig. 7 shows the responses of the pure In_2O_3 (Type 1) and the In_2O_3–ZnO ($r = 0.67$, Type 2) films against NO_x, CO, and NO_2 gases at 150 °C. In fact, both pure In_2O_3 and In_2O_3–ZnO ($r = 0.67$) composite films showed no response to 10 ppm CO gas. Thus, the response of CO was not noticed in Fig. 7. On the other hand, NO_2 gas showed significant interfering effect to both pure In_2O_3 and In_2O_3–ZnO ($r = 0.67$) films, and the In_2O_3–ZnO film even showed a higher response to NO_2 than NO_x. Further work on the effect of the doping amount of ZnO on the sensing performance of In_2O_3–ZnO film towards NO_2 is under investigation.

Finally, the long-term stability of In_2O_3–ZnO film ($r = 0.67$) was investigated by examining the response of the In_2O_3–ZnO ($r = 0.67$) film to 10 ppm NO_x, three cycles per once and once per week, for one month. After the test, the electrode was stored in a box, exposed to the ambient air at room temperature with a relative humidity of

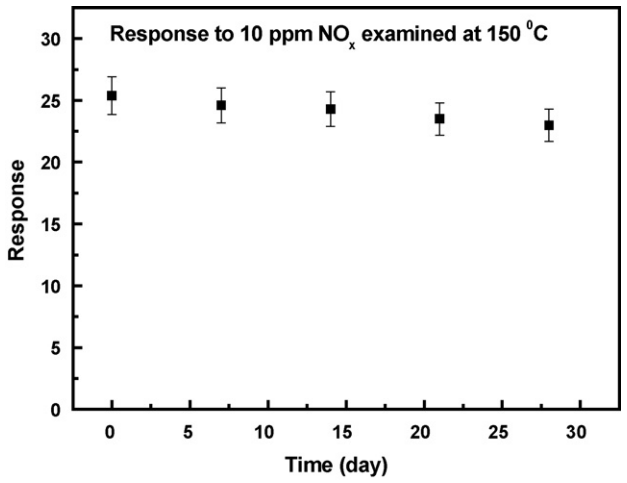

Fig. 8. The responses of In_2O_3–ZnO film to 10 ppm NO_x at 150 °C obtained for different periods.

45%. As shown in Fig. 8, the sensor response remained about 90% after one month use.

4. Conclusions

The In_2O_3–ZnO composite films were synthesized and their NO_x gas sensing characteristics were studied. After incorporating ZnO into In_2O_3 film, the formation of the rhombohedral phase of In_2O_3 and morphological changes were noticed. Besides, with suitable amount of ZnO into the In_2O_3 films ($0.33 \leqq r \leqq 0.67$), the responses of the resulted composite films to NO_x gas at low temperature ($\leqq$200 °C) were increased. However, as the content of ZnO was increased ($r \geqq 1.00$), the response of the resultant composite film decreased dramatically due to the morphological change. The results suggest that the gas sensors based on the In_2O_3–ZnO composite films have the potential to become candidate for environmental monitoring.

Acknowledgements

This work was sponsored by the National Research Council of Taiwan under grant numbers NSC 97-2220-E-006-008, NSC 98-2220-E-006-008, and NSC 98-EC-17-A-02-S2-0125.

References

[1] L. Kreuzer, C. Patel, Nitric oxide air pollution: detection by optoacoustic spectroscopy, Science 173 (1971) 182–187.
[2] N.L.R. Han, J.S. Ye, A.C.H. Yu, F.S. Sheu, Differential mechanisms underlying the modulation of delayed-rectifier K^+ channel in mouse neocortical neurons by nitric oxide, J. Neurophysiol. 95 (2006) 2167–2178.
[3] M.J. Ratnawati, R.L. Henry, P.S. Thomas, Exhaled breath condensate nitrite/nitrate and pH in relation to pediatric asthma control and exhaled nitric oxide, Pediatr. Pulmonol. 41 (2006) 929–936.
[4] F.M. Delen, J.M. Sippel, M.L. Osborne, A. Law, N. Thukkani, W.E. Holden, Increased exhaled nitric oxide in chronic bronchitis—comparison with asthma and COPD, Chest 117 (2000) 695–701.
[5] A. Forleo, L. Francioso, M. Epifani, S. Capone, A.M. Taurino, P. Siciliano, NO_2-gas-sensing properties of mixed In_2O_3–SnO_2 thin films, Thin Solid Films 490 (2005) 68–73.
[6] C.S. Rout, K. Ganesh, A. Govindaraj, C.N.R. Rao, Sensors for the nitrogen oxides, NO_2, NO and N_2O, based on In_2O_3 and WO_3 nanowires, Appl. Phys. A 85 (2006) 241–246.
[7] J. Hu, F. Zhu, J. Zhang, Hao Gong, A room temperature indium tin oxide/quartz crystal microbalance gas sensor for nitric oxide, Sens. Actuators B: Chem. 93 (2003) 175–180.
[8] D. Zhang, C. Zuqin Liu, T. Li, Z. Tang, S. Liu, B. Han, C. Lei, Zhou, Detection of NO_2 down to ppb levels using individual and multiple In_2O_3 nanowire devices, Nano Lett. 4 (2004) 1919–1924.
[9] M. Epifani, E. Comini, J. Arbiol, R. Díaz, N. Sergent, T. Ragnier, P. Siciliano, G. Faglia, J.R. Morante, Chemical synthesis of In_2O_3 nanocrystals and their application in highly performing ozone-sensing devices, Sens. Actuators B: Chem. 130 (2008) 483–487.
[10] G. Korotcenkov, A. Cerneavschi, V. Brinzari, A. Vasiliev, M. Ivanov, A. Cornet, J.R. Morante, A. Cabot, J. Arbiol, In_2O_3 films deposited by spray pyrolisis as a material for ozone gas sensors, Sens. Actuators B: Chem. 99 (2004) 297–303.
[11] N. Du, H. Zhang, B. Chen, X. Ma, Z. Liu, J. Wu, D. Yang, Porous indium oxide nanotubes: layer-by-layer assembly on carbon-nano-tube templates and application for room-temperature NH_3 gas sensors, Adv. Mater. 19 (2007) 1641–1645.
[12] T. Waitz, T. Wanger, T. Sauerwald, C.D. Kohl, M. Tiemann, Ordered mesoporous In_2O_3: synthesis by structure replication and application as a methane gas sensor, Adv. Funct. Mater. 19 (2009) 653–661.
[13] V.D. Kapse, S.A. Ghosh, G.N. Chaudhari, F.C. Raghuwanshi, Nanocrystalline In_2O_3-based H_2S sensors operable at low temperatures, Talanta 76 (2008) 610–616.
[14] C.M. Chimbeu, M. Lumbreras, M. Siadat, J. Schoonman, Detection of pollutant gases using electrostatic sprayed indium oxide and tin-doped indium oxide, Mater. Chem. Phys. 114 (2009) 933–938.
[15] C.Y. Lin, P.C. Nien, W.Y. Feng, C.W. Lin, J.J. Tunney, K.C. Ho, Chemiresistive NO gas sensor based on zinc oxide nanorods, J. Bionanosci. 2 (2008) 102–108.
[16] P.S. Cho, K.W. Kim, J.H. Lee, NO_2 sensing characteristics of ZnO nanorods prepared by hydrothermal method, J. Electroceram. 17 (2006) 975–978.
[17] J.H. Yu, G.M. Choi, Electrical and CO gas sensing properties of ZnO–SnO_2 composites, Sens. Actuators B: Chem. 52 (1998) 251–256.
[18] T. Miyata, T. Minami, K. Shimokawa, T. Kakumu, M. Ishii, New materials consisting of multicomponent oxides for thin-film gas sensors, J. Electrochem. Soc. 144 (1997) 2432–2436.

[19] L. Vayssieres, Growth of arrayed nanorods and nanowires of ZnO from aqueous solutions, Adv. Mater. 15 (2003) 464–466.
[20] A. Gurlo, M. Ivanovskaya, N. Bârsan, M. Schweizer-Berberich, U. Weimar, W. Göpel, A. Diéguez, Grain size control in nanocrystalline In_2O_3 semiconductor gas sensors, Sens. Actuators B: Chem. 44 (1997) 327–333.
[21] I. Sayago, J. Gutiérrez, L. Arés, J.I. Robla, M.C. Horrillo, J. Getino, J. Rino, J.A. Agapito, The effect of additives in tin oxide on the sensitivity and selectivity to NO_x and CO, Sens. Actuators B: Chem. 26–27 (1995) 19–23.
[22] B. Ruhland, T. Becker, G. Müller, Gas–kinetic interactions of nitrous oxides with SnO_2 surfaces, Sens. Actuators B: Chem. 50 (1998) 85–94.
[23] A. Cabot, A. Marsal, J. Arbiol, J.R. Morante, Bi_2O_3 as a selective sensing material for NO detection, Sens. Actuators B: Chem. 99 (2004) 74–89.
[24] T.J. Koplin, M. Siemons, C. Océn-Valéntin, D. Sanders, U. Simon, Workflow for high throughput screen of gas sensing materials, Sensors 6 (2006) 298–307.
[25] C.Y. Wang, M. Ali, T. Kups, C.C. Röhlig, V. Cimalla, T. Stauden, O. Ambacher, NO_x sensing properties of In_2O_3 nanoparticles prepared by metal organic chemical vapor deposition, Sens. Actuators B: Chem. 130 (2008) 589–593.
[26] L. Francioso, A. Forleo, S. Capone, M. Epifani, A.M. Taurino, P. Siciliano, Nanostructured In_2O_3–SnO_2 sol–gel thin film as material for NO_2 detection, Sens. Actuators B: Chem. 114 (2006) 646–655.
[27] C. Liewhiran, S. Phanichphant, Influence of thickness on ethanol sensing characteristics of doctor-bladed thick film from flame made ZnO nanoparticles, Sensors 7 (2007) 185–201.
[28] F. Palmgren, R. Berkowicz, O. Hertel, E. Vignati, Effects of reduction of NO_x on the NO_2 levels in urban streets, Sci. Total Environ. 189–190 (1996) 409–415.

Biographies

Chia-Yu Lin received his B.S. degree in Chemical Engineering from the National Cheng Kung University, Tainan, Taiwan, in 2003. He received his M.S. degree in Chemical Engineering from the National Taiwan University, Taipei, Taiwan in 2005. Currently, he is a fourth-year Ph.D. student in the Department of Chemical Engineering at the National Taiwan University. His research interest mainly surrounds nanomaterials for chemiresistive-type gas sensor and electrochemical biosensor applications.

Yueh-Yuan Fang received her B.S. degree in Electrical Engineering from the National Central University, Taoyuan, Taiwan, in 2006. Now, she is a Ph.D. student in second grade in Biomedical Engineering at the National Taiwan University. Her current research interests include electromyography signal processing, bio nano/micro electro-mechanical systems processing, polymer light-emitting diode, as well as SPR sensors.

Chii-Wann Lin received his B.S. from the Department of Electrical Engineering, National Cheng-Kung University in 1984. He then started his career in biomedical engineering with a M.S. degree from the Graduate Institute of Biomedical Engineering, National Yang-Ming University in 1986. After two years of military service, he attended the Case Western Reserve University and received his Ph.D. degree in Biomedical Engineering in January 1993. Before his return to Taiwan, he had been a research associate in the Neurology Department, CWRU from January 1993 to August 1993. He worked in the Center for Biomedical Engineering, College of Medicine, National Taiwan University from September 1993 to August 1998. He is now a professor in the Graduate Institute of Biomedical Engineering and holds joint appointments in both the Department of Electrical Engineering and the Institute of Applied Mechanics, National Taiwan University. He is also a member of IEEE EMBS, IFMBE, and Chinese BMES. He will hold the position of president of the Taiwan Association of Chemical Sensors from 2008 to 2010. His research interests include biomedical microsensors, optical biochip, surface plasmon resonance, bio-plasmonics, nano-medicine, and personal e-health system.

James J. Tunney obtained his Ph.D. in Chemistry in 1995 from the University of Ottawa, Canada. He joined the National Research Council of Canada in 1996 first as a Post-Doctoral Fellow, and later as a Research Officer. Since 2006, he has also served as a Competency Leader for Organic Materials at NRC-ICPET. His research interests include the use of thin and thick film technology applied to chemical sensing.

Kuo-Chuan Ho received his B.S. and M.S. degrees in Chemical Engineering from the National Cheng Kung University, Tainan, Taiwan, in 1978 and 1980, respectively. In 1986, he received his Ph.D. degree in Chemical Engineering at the University of Rochester. The same year he joined PPG Industries, Inc., first as a Senior Research Engineer and then, from 1990 until 1993, as a Research Project Engineer. He has worked on the electrochemical properties of various electrode materials, with emphasis on improving the performances of sensor devices. Following a six-year industrial career at PPG Industries, Inc., he joined his alma mater at National Cheng Kung University in 1993 as an Associate Professor in the Chemical Engineering Department. In 1994, he moved to the Department of Chemical Engineering at the National Taiwan University. Currently, he is a Professor jointly appointed by the Department of Chemical Engineering and Institute of Polymer Science and Engineering at National Taiwan University.